Hindawi Publishing Corporation
Advances in Materials Science and Engineering
Volume 2015, Article ID 616980, 8 pages
http://dx.doi.org/10.1155/2015/616980

Research Article

Prediction of Chloride Penetration into Hardening Concrete

Wei-Jie Fan and Xiao-Yong Wang

Department of Architectural Engineering, Kangwon National University, Chuncheon-si 200 701, Republic of Korea

Correspondence should be addressed to Xiao-Yong Wang; wxbrave@kangwon.ac.kr

Received 30 April 2015; Revised 29 June 2015; Accepted 1 July 2015

Academic Editor: Antônio G. B. de Lima

In marine and coastal environments, penetration of chloride ions is one of the main mechanisms causing concrete reinforcement corrosion. Currently, most of experimental investigations about submerged penetration of chloride ions are started after the four-week standard curing of concrete. The further hydration of cement and reduction of chloride diffusivity during submerged penetration period are ignored. To overcome this weak point, this paper presents a numerical procedure to analyze simultaneously cement hydration reaction and chloride ion penetration process. First, using a cement hydration model, degree of hydration and phase volume fractions of hardening concrete are determined. Second, the dependences of chloride diffusivity and chloride binding capacity on age of concrete are clarified. Third, chloride profiles in hardening concrete are calculated. The proposed numerical procedure is verified by using chloride submerged penetration test results of concrete with different mixing proportions.

1. Introduction

The ingress of chloride ions constitutes a major source of durability problems affecting reinforced concrete structures which are exposed to marine environments. Once a sufficient quantity of chloride ions has accumulated around the embedded steel, pitting corrosion of the metal is liable to occur unless the environmental conditions are strongly anaerobic. In the design of concrete structures, the influence of chloride ingress on service life must be considered [1].

The literature is rich in papers dealing with modeling of chloride attack of concrete. Papadakis [2, 3] proposes chemical reaction equations for silica fume, low calcium fly ash, and high calcium fly ash blended concrete. Using the volumetric relations calculated chemical reaction equations, porosity and chloride diffusivity of hardened concrete are determined. Han [4] proposes a modified diffusion coefficient that considers the effect of chloride binding and evaporable water on the diffusion coefficient. Based on the modified diffusion coefficient, numerical methods are used to estimate chloride concentration according to concrete depth and external and internal conditions. Spiesz [5, 6] analyzed chloride penetration profiles during rapid chloride migration tests. The diffusion flux during migration tests is shown to be insignificant compared to the electrical migration flux. However, it should be noticed that current models [2–6] focus on chloride penetration into fully hardened concrete.

Currently, most of experimental investigations about submerged penetration of chloride ions are started after the four-week standard curing of concrete [7–9]. After concrete with four-week initial curing, cement hydration reaction will proceed continuously [10, 11]. Hence four-week initial cured concrete is not fully hardened concrete, but slowly hardening concrete. After four-week initial curing of concrete, chloride diffusivity continuously decreases with the prolongation of curing period [7–9]. For chloride penetration into hardening concrete, cement hydration and chloride ingress will occur simultaneously, and current chloride penetration models [2–6] are not valid for hardening concrete.

To overcome the weak points of current models [2–6], this paper presents a numerical procedure to analyze simultaneously cement hydration reaction and chloride ion penetration process. By combining hydration model with chloride ingress model, the dependences of chloride diffusivity and chloride binding capacity on age of concrete are clarified. Furthermore, chloride profiles in hardening concrete are determined.

The original contributions of this paper are shown as follows: first, evaluate the phase volume fractions of hardening concrete by using a kinetic hydration model; second,

predict the evolution of chloride diffusivity by using capillary porosity in cement paste; third, consider interactions between cement hydration and chloride penetration. The influences of curing ages on chloride attack durability are clarified.

2. Cement Hydration Model

Tomosawa [12] proposed a shrinking-core model to model the hydration of Portland cement. However, Tomosawa's original model does not consider the effects of capillary water on cement hydration and is only valid for low strength or ordinary strength concrete with higher water to binder ratios. Recently, to overcome weak points of Tomosawa's model, Wang [10, 11] revised Tomosawa's model to consider effects of water to binder ratio, mineral compositions, and capillary water concentrations on cement hydration process. The revised model is valid for concrete with different strengths, different cement mineral compositions, and different curing methods.

The proposed blended cement hydration model by Wang [10, 11] is valid for not only blended cement but also Portland cement. Using the hydration model, hydration degree of cement and reaction degree of mineral admixtures are determined. Furthermore, the age dependent properties of hardening concrete are evaluated using reaction degrees of binders.

The proposed blended cement hydration model by Wang [10, 11] consists of two parts, that is, cement hydration model and mineral admixtures reaction model. Because this paper mainly focuses on hydration related properties of Portland cement concrete, only cement hydration model is shown. Mineral admixtures reaction model is not shown in this paper.

This revised Portland cement hydration model by Wang [10, 11] is expressed as a single equation consisting of three coefficients: k_d the reaction coefficient in the induction period; D_e the effective diffusion coefficient of water through the C–S–H gel; and k_{ri} a coefficient of the reaction rate of mineral compound of cement as shown in the following equations:

$$\frac{d\alpha_i}{dt} = \frac{3\left(S_w/S_0\right)\rho_w C_{w-\text{free}}}{\left(\nu + w_g\right) r_0 \rho_c} \cdot \frac{1}{\left(1/k_d - r_0/D_e\right) + \left(r_0/D_e\right)\left(1-\alpha_i\right)^{-1/3} + \left(1/k_{ri}\right)\left(1-\alpha_i\right)^{-2/3}} \tag{1a}$$

$$\alpha = \frac{\sum_{i=1}^{4} \alpha_i g_i}{\sum_{i=1}^{4} g_i}, \tag{1b}$$

where α_i ($i = 1, 2, 3$, and 4) represents reaction degree of mineral compounds of cement C_3S, C_2S, C_3A, and C_4AF, respectively; α is the degree of cement hydration and can be calculated from the weight fraction of mineral compound g_i and reaction degree of mineral compound α_i; ν is the stoichiometric ratio by mass of water to cement (= 0.25); w_g is the physically bound water in C–S–H gel (= 0.15); ρ_w is the density of water; ρ_c is the density of the cement; $C_{w-\text{free}}$ is the amount of water at the exterior of the C–S–H gel; r_0 is the radius of unhydrated cement particles; S_w is the effective surface area of the cement particles in contact with water; and S_0 is the total surface area if the surface area develops unconstrained.

The reaction coefficient k_d is assumed to be a function of the degree of hydration as shown in (2), where B and C are the coefficients determining this factor; B controls the rate of the initial shell formation and C controls the rate of the initial shell decay:

$$k_d = \frac{B}{\alpha^{1.5}} + C\alpha^3. \tag{2}$$

The effective diffusion coefficient of water is affected by the tortuosity of the gel pores as well as the radii of the gel pores in the hydrate. This phenomenon can be described as a function of the degree of hydration and is expressed as follows:

$$D_e = D_{e0} \ln\left(\frac{1}{\alpha}\right). \tag{3}$$

In addition, free water in the capillary pores is depleted as hydration of cement minerals progresses. Some water is bound in the gel pores, and this water is not available for further hydration, an effect that must be taken into consideration in every step of the progress of the hydration. Therefore, the amount of water in the capillary pores $C_{w-\text{free}}$ is expressed as a function of the degree of hydration in the previous step as shown in the following:

$$C_{w-\text{free}} = \frac{W_0 - 0.4 * \alpha * C_0}{W_0}, \tag{4}$$

where C_0 and W_0 are the mass fractions of cement and water in the mix proportion.

The effect of temperature on these reaction coefficients is assumed to follow Arrhenius's law as shown in

$$\begin{aligned} B &= B_{20} \exp\left(-\beta_1\left(\frac{1}{T} - \frac{1}{293}\right)\right) \\ C &= C_{20} \exp\left(-\beta_2\left(\frac{1}{T} - \frac{1}{293}\right)\right) \\ k_{ri} &= k_{ri20} \exp\left(-\frac{E}{R}\left(\frac{1}{T} - \frac{1}{293}\right)\right) \\ D_e &= D_{e20} \exp\left(-\beta_3\left(\frac{1}{T} - \frac{1}{293}\right)\right), \end{aligned} \tag{5}$$

where β_1, β_2, E/R, and β_3 are temperature sensitivity coefficients and B_{20}, C_{20}, k_{ri20}, and D_{e20} are the values of B, C, k_{ri}, and D_e at 20°C.

Using reaction degree of cement, the phase volume fractions of hardening cement paste (sealed curing) can be determined as follows:

$$V_1 = \frac{C_0}{\rho_c}(1-\alpha) \tag{6}$$

Table 1: Coefficients of cement hydration model.

B_{20} (cm/h)	C_{20} (cm/h)	k_{rC_3S20} (cm/h)	k_{rC_2S20} (cm/h)	k_{rC_3A20} (cm/h)	k_{rC_4AF20} (cm/h)	D_{e20} (cm^2/h)	β_1 (K)	β_2 (K)	β_3 (K)	E/R (K)
8.09×10^{-9}	0.02	9.03×10^{-6}	2.71×10^{-7}	1.35×10^{-6}	6.77×10^{-8}	8.62×10^{-10}	1000	1000	7500	5400

$$V_2 = W_0 - 0.4 * \alpha * C_0 \tag{7}$$

$$V_3 = 0.15 * \alpha * C_0 \tag{8}$$

$$V_4 = W_0 - 0.4 * \alpha * C_0 + 0.15 * \alpha * C_0 \tag{9}$$

$$V_5 = 0.0625 * \alpha * C_0 \tag{10}$$

$$V_6 = W_0 - 0.4 * \alpha * C_0 + 0.0625 * \alpha * C_0 \tag{11}$$

$$V_7 = W_0 - 0.4 * \alpha * C_0 + 0.0625 * \alpha * C_0 + 0.15 * \alpha * C_0, \tag{12}$$

where V_1, V_2, V_3, V_4, V_5, V_6, and V_7 are the volume of anhydrous cement, capillary water, gel water, evaporable water (the sum of capillary water and gel water), chemical shrinkage, capillary porosity (the sum of capillary water and chemical shrinkage), and total porosity (the sum of capillary porosity and gel water), respectively.

On the basis of degree of reactions of mineral compounds of cement, the parameters of hydration model are calibrated and shown in Table 1. Using this Portland cement hydration model, Wang [10, 11] evaluated the heat evolution rate, adiabatic temperature rise, compressive strength development, and thermal stress development in both ordinary strength concrete and high strength concrete.

3. Chloride Penetration Model

3.1. Governing Equation of Chloride Diffusion. Due to the existing concentration gradient between the exposed surface and the pore solution of the cement matrix (diffusion driving force), chloride ions enter the concrete by ionic diffusion. This process is often described by Fick's 1st law of diffusion as follows [13–16]:

$$J_c = -D_c \frac{\partial C_f}{\partial x}, \tag{13}$$

where J_c is the flux of chloride ions due to diffusion (kg/m^2·s); D_c is the effective diffusion coefficient when the concentration is expressive in kilograms per cubic meter of pore solution (m^2/s); C_f is free chloride concentration (kg/m^3 of pore solution) at depth x (m).

The chloride mass conservation in saturated concrete can be described by Fick's second law, as follows [15–20]:

$$\frac{\partial C_t}{\partial t} = -\nabla \cdot J_c, \tag{14}$$

where C_t is the total chloride concentration (kg/m^3 of concrete) and t is time (s).

Chlorides present in concrete are generally classified into free chloride and bound chloride. Free chlorides are dissolved in the pore liquid and exist in a freely mobile form. Bound chlorides consist of adsorbed chloride and solid phase chloride. Bound chlorides do not move at ordinary concentration gradient. The total, bound, and free chloride concentrations in concrete are related as follows [15, 16]:

$$C_t = C_b + V_4 * C_f, \tag{15}$$

where C_b is the concentration of bound chlorides (kg/m^3 of concrete). The evaporable water contents V_4 can be determined from hydration model using (9).

By substituting (15) into (14), the following modified Fick's second law equation can be obtained as follows [15, 16]:

$$\frac{\partial C_f}{\partial t} = \frac{\partial}{\partial x}\left(\frac{D_c}{V_4 + \partial C_b/\partial C_f}\frac{\partial C_f}{\partial x}\right), \tag{16a}$$

where $\partial C_b/\partial C_f$ is the binding capacity of the concrete binder (m^3 of pore solution/m^3 of concrete). As shown in (16a), chloride penetration process relates to chloride diffusivity, binding capacity, and evaporable water contents of concrete. Equations (15) and (16a) consider the mass conservation among total chloride, bound chloride, and free chloride.

The initial and boundary conditions used for the analysis are shown as follows:

$$\begin{aligned} &\text{For } t = 0: \quad C_f = C_0 \quad \text{at } x > 0 \\ &\text{For } t \geq 0: \quad C_f = C_s \quad \text{at } x = 0 \\ &\qquad\qquad\quad\; C_f = C_0 \quad \text{at } x = L, \end{aligned} \tag{16b}$$

where C_0 is the concentration of chlorides present in the pore solution before concrete is exposed to a salt solution, C_s is the chloride concentration of salt solution in contact with the outer surface, and L is the thickness of the member.

3.2. Chloride Diffusion Coefficient and Binding Isotherm. At the macroscopic level, concrete is a composite material consisting of discrete aggregates dispersed in a continuous cement paste matrix. The diffusion of chloride ions mainly through capillary pore of cement paste and diffusivity of aggregate particle inclusions is assumed to be zero [15, 16]. For hardening concrete, the effective diffusion coefficient D_c can be determined from capillary porosity of paste phase and aggregate contents in concrete as follows:

$$D_c(t) = A_1 * \left(\phi_{\text{paste}}\right)^{A_2} \frac{2\left(1 - V_a\right)}{2 + V_a} \tag{17a}$$

$$\phi_{\text{paste}} = \frac{V_6}{C_0/\rho_c + W_0}, \tag{17b}$$

where A_1 and A_2 are relation coefficients between capillary porosity and chloride diffusivity, ϕ_{paste} is the capillary porosity in paste, and V_a is the volume of aggregate in concrete. The former item $A_1 * (V_6)^{A_2}$ considers effect of hydration of cement paste on chloride diffusivity and the latter item $2(1-V_a)/(2+V_a)$ considers effect of additions of aggregate on chloride diffusivity. As shown in (17b), the capillary porosity in paste ϕ_{paste} can be determined from capillary porosity in concrete and paste volume in concrete. It should be noticed that (17a) and (17b) are original works of authors.

Diffusing chloride ions are bound physically and chemically onto pore surfaces within cement matrix [8, 11]. Due to the reactions between chloride ion and C_3A or C_4AF, resulting in the formation of Friedel's salt and its analogues, the contents of C_3A and C_4AF in cement dominate chemical binding of chloride ion. On the other hand, calcium silicate hydrate (CSH) gel is the main hydration product of C_3S and C_2S. Due to the adsorption of chloride ion to the CSH, chloride ions will be physically bound in CSH. Hence, C_3S and C_2S dominate physical binding.

Chloride binding isotherms describe the relationships between free and bound chlorides in concrete at a given temperature. They are unique to each cementitious system since they are influenced by the components making up that system, such as C_3A content, supplementary cementing materials, and pH of the pore solution. They are also influenced by the environmental conditions surrounding the system such as temperature.

Langmuir isotherm and Freundlich isotherm are frequently used to describe the nonlinear binding essence of chloride ions [9, 11]. The Langmuir isotherm, derived from physical chemistry, is assuming monolayer adsorption, which explains that the slope of the isotherm curve at high concentrations approaches zero. LuPing et al. [9] suggested that monolayer adsorption occurs at low concentrations (which is described better by Langmuir isotherm), but that adsorption becomes more complex at concentrations higher than 0.05 M and is described better by the Freundlich isotherm. The difference between the Freundlich and Langmuir isotherms is their behavior at high concentrations. It was found by LuPing et al. [9] that the Freundlich equation fits the data very well in a range of free chloride concentrations from 0.01 to 1 M. This range covers the two most important magnitude orders of free chloride concentration in sea water. Considering the wide concentration range of Freundlich isotherm, in this paper, Freundlich isotherm is used to describe the nonlinear binding essence of chloride ions.

The equation of Freundlich binding isotherm (nonlinear binding isotherm) is shown as follows [8, 15, 16]:

$$C_b = F_1 * (1 - V_7) * \left(C_f\right)^{F_2}, \tag{18}$$

where F_1 and F_2 are relation coefficients between free chloride and bound chloride. The total porosity of concrete V_7 in (18) can be determined from hydration model using (12). The item $(1 - V_7)$ in (18) means the volume of solid phase in concrete. For OPC concrete, the relation coefficients between free chloride and bound chloride, that is, F_1 and F_2, are assumed as 2.5 and 0.5, respectively [8]. These relation coefficients do not vary with mixing proportions or curing ages. The influence of porosity on chloride binding isotherm is shown in Figure 1. As shown in this figure, with the proceeding of cement hydration, hydration products will be produced, the porosity of concrete will decrease, and chloride ions binding capacity will be enhanced.

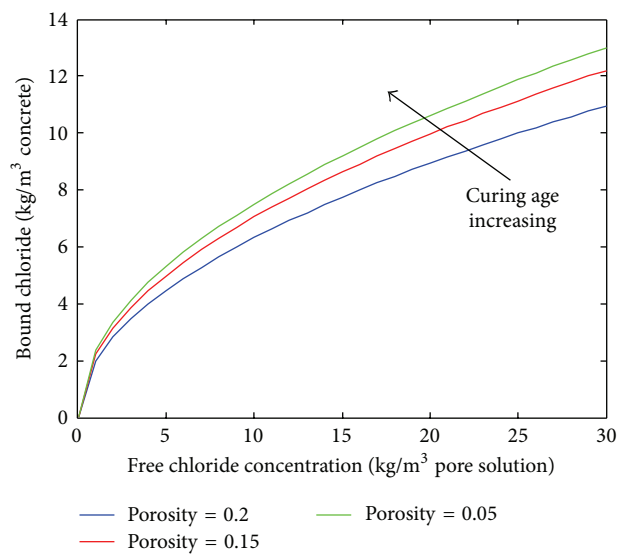

Figure 1: Influence of curing age on binding isotherm of concrete.

3.3. Summary of Proposed Cement Hydration-Chloride Penetration Model. The proposed numerical procedure considers the interactions between cement hydration and chloride penetrations. The flowchart of numerical procedure is shown in Figure 2 and summarized as follows.

First, using a cement hydration model, degree of hydration and phases volume fractions of hardening concrete, such as evaporable water content, capillary porosity, and total porosity, are determined.

Second, the dependences of chloride diffusivity and chloride binding capacity on age of concrete are clarified. Chloride diffusivity of hardening concrete is calculated considering capillary porosity evolution in cement paste and aggregate dilution effect. Chloride binding is described using nonlinear binding isotherm.

Third, chloride profiles in hardening concrete are calculated. Governing equation of chloride diffusion ((16a) and (16b)) in space is a boundary-value problem and in time is an initial-value problem. In this paper, a one-dimensional finite element method is adopted to solve this equation. For numerical time integration part, the Galerkin method is used to confirm the stability of numerical integration [10, 11].

4. Verification of Proposed Model

Experimental results about chloride diffusivity and total chloride concentrations in [8] are used to verify the proposed model. Chloride diffusivity and chloride concentration profiles of concrete specimens with different mixing proportions

Table 2: Chemical compositions of cement.

Chemical composition (mass %)							Physical properties	
SiO_2	Al_2O_3	Fe_2O_3	CaO	MgO	SO_3	Lg.loss	Specific gravity (g/cm^3)	Blaine (cm^2/g)
21.96	5.27	3.11	63.41	2.13	1.96	0.79	3.16	3214

Table 3: Mixing proportions of concrete.

Water to cement ratio	Water (kg/m^3)	Cement (kg/m^3)	Sand (kg/m^3)	Gravel (kg/m^3)	Super plasticizer (% of binder)
0.37	168	454	767	952	1%
0.42	168	400	787	976	0.9%
0.47	168	357	838	960	0.85%

are measured at different curing ages. Normal Portland cement was used to make concrete specimens. The chemical compositions and physical properties of cement are shown in Table 2. Using Bogue equations, the mineral compositions C_3S, C_2S, C_3A, and C_4AF of used cement are determined as 45.33%, 28.76%, 8.14%, and 10.46%, respectively. Concrete specimens with different water to cement ratios, that is, 0.47, 0.42, and 0.37, were prepared. The mixing proportions of concrete are shown in Table 3. The sand to aggregate ratio of concrete specimens is about 0.45.

Experimental program for chloride diffusion coefficient [8]: concrete cylinder specimens are cured in submerged conditions. At the age of 28 days, 90 days, 180 days, and 270 days, chloride diffusion coefficients are measured using electrical accelerate method. The sizes of cylinder specimens of chloride diffusion coefficients tests are 100 mm $*$ 50 mm. The diffusion cell and experimental setup are provided in ASTMC 1202. The cathode of electrolyte is 0.5 Mole NaCl solution and the anode electrolyte is saturated $Ca(OH)_2$. The applied voltage is 30 V and duration time is 8 hours. After accelerated test, silver nitrate solution (0.1 N, $AgNO_3$) is used as an indicator to measure penetration depth and the diffusion coefficient is calculated through penetration depth of chloride ions.

Experimental program for chloride penetration profile [8]: after 28 days of curing, the specimens are submerged in 3.5% NaCl solution for 6 months. The specimens were coated with resin except for upside surface for 1-dimensional intrusion of chloride ions. Acid-soluble chloride contents (total chloride contents) are measured for different depths.

Using the proposed hydration model, the hydration related properties of concrete are shown in Figure 3. As shown in Figure 3(a), with the decreasing of water to binder ratio, due to limitation of capillary water and available space for deposition of hydration products, the reaction degree of cement will decrease. As shown in Figure 3(b), because of filling effect of cement hydration products, capillary porosity of cement paste decreases with the proceeding of cement hydration. As shown in Figure 3(c), due to the consumption of mixing water, the evaporable water content in concrete decreases with the prolongation of curing age. At a given curing age, concrete with a lower water to cement ratio shows lower capillary porosity and evaporable water content.

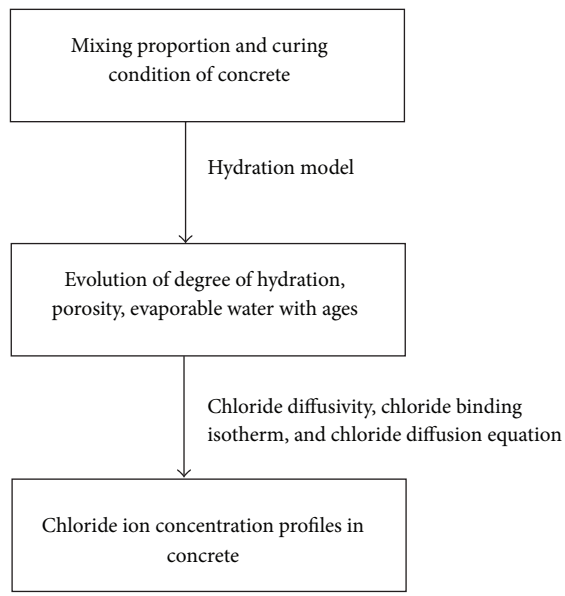

Figure 2: Flowchart of proposed numerical procedure.

Figure 4 presents the phase volume fractions of cement paste with water to binder ratio 0.37. As shown in this figure, with the proceeding of hydration reaction, the volumes of cement decrease, and the volumes of reaction products from cement hydration increase. Because of losses in the capillary water, decreasing of available deposition spaces for hydration products, and changing of hydration rate determining process to a diffusion-controlled stage, the rate of hydration becomes slower.

The relation between capillary porosity in cement paste and chloride diffusion coefficients is shown in Figure 5(a). As shown in this figure, for concrete with different water to cement ratios and at different curing ages, the relation between chloride diffusion coefficients and capillary porosity is similar. This is because, compared with gel pore in calcium silica hydrate, the pore size of capillary pore is much larger,

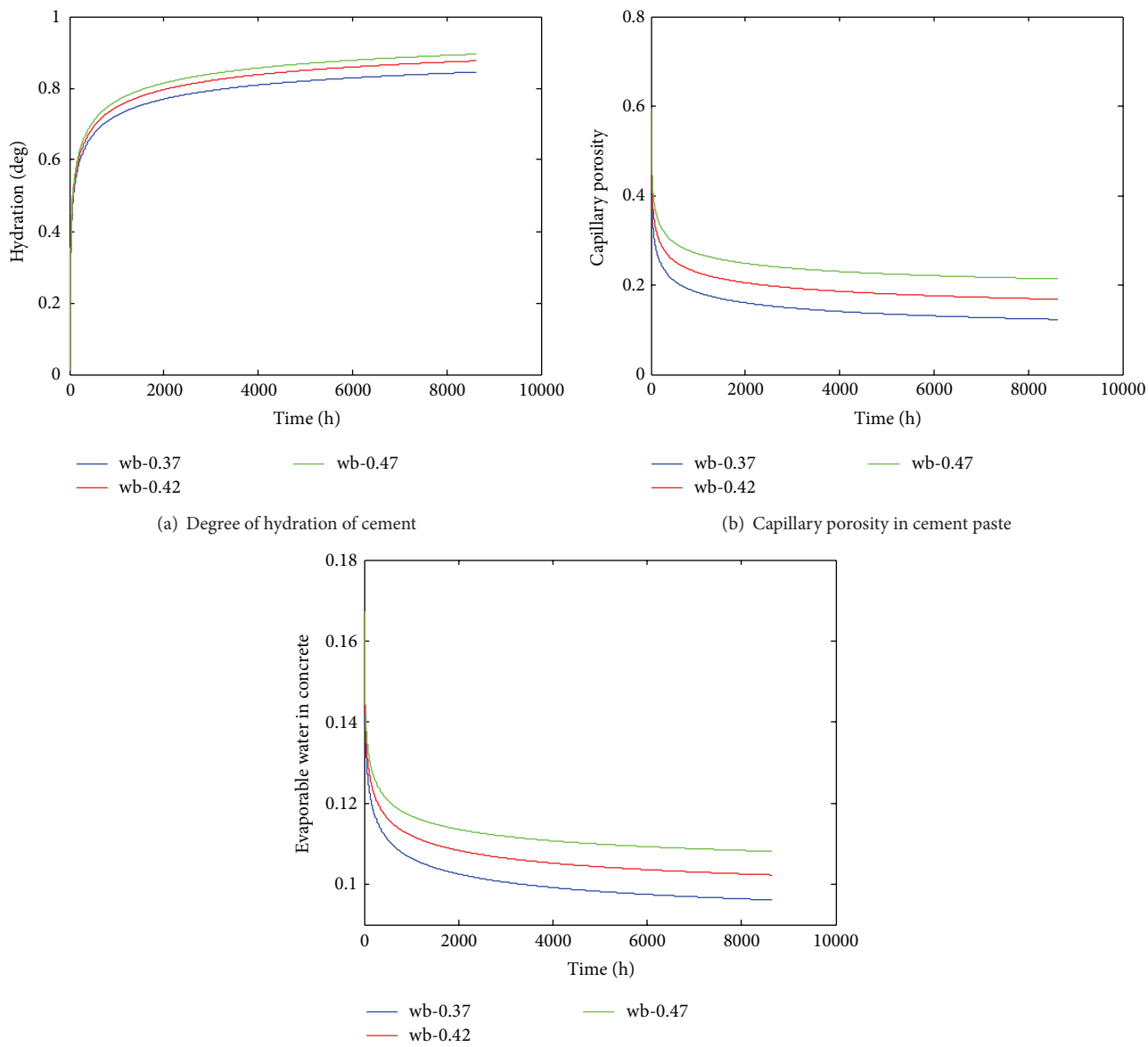

(a) Degree of hydration of cement

(b) Capillary porosity in cement paste

(c) Evaporable water in concrete

Figure 3: Hydration related properties of concrete.

and capillary pore is main penetration path of chloride ions. Chloride diffusion coefficients almost linearly increase with the increase of capillary porosity in paste. Hence, capillary porosity in paste is an effective index to determine chloride diffusion coefficient. The regression coefficients of A_1 and A_2 in (17a) are given as $3.63e-10$ and 1.15, respectively. As shown in Figure 5(b), from 28 days to 270 days, with the increasing of curing age, due to the reduction of capillary porosity, the chloride diffusion coefficients decease almost 40%. The proposed model can reflect the dependences of chloride diffusion coefficients on curing age and water to cement ratios.

The calculated total chloride concentration profiles are shown in Figure 6. The calculated results generally agree with experimental results. With the increasing of water to cement ratios, at the same depth, due to the reductions of chloride diffusion coefficients, the chloride ions concentration will decrease.

5. Conclusions

This paper presents a numerical procedure to analyze chloride penetration into hardening concrete. The simultaneous cement hydration reaction and chloride ion penetration process are modeled. First, using a cement hydration model, degree of hydration and phases volume fractions of hardening concrete, such as evaporable water content, capillary porosity, and total porosity, are determined. Second, the

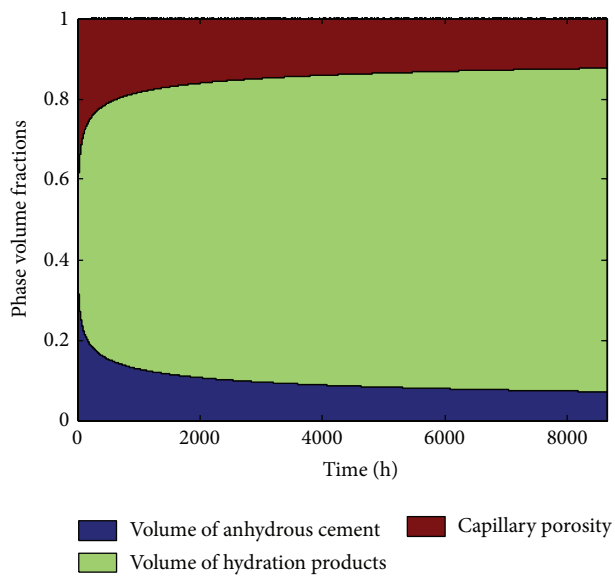

Figure 4: Phase volume fractions of hydrating paste (water to cement ratio 0.37).

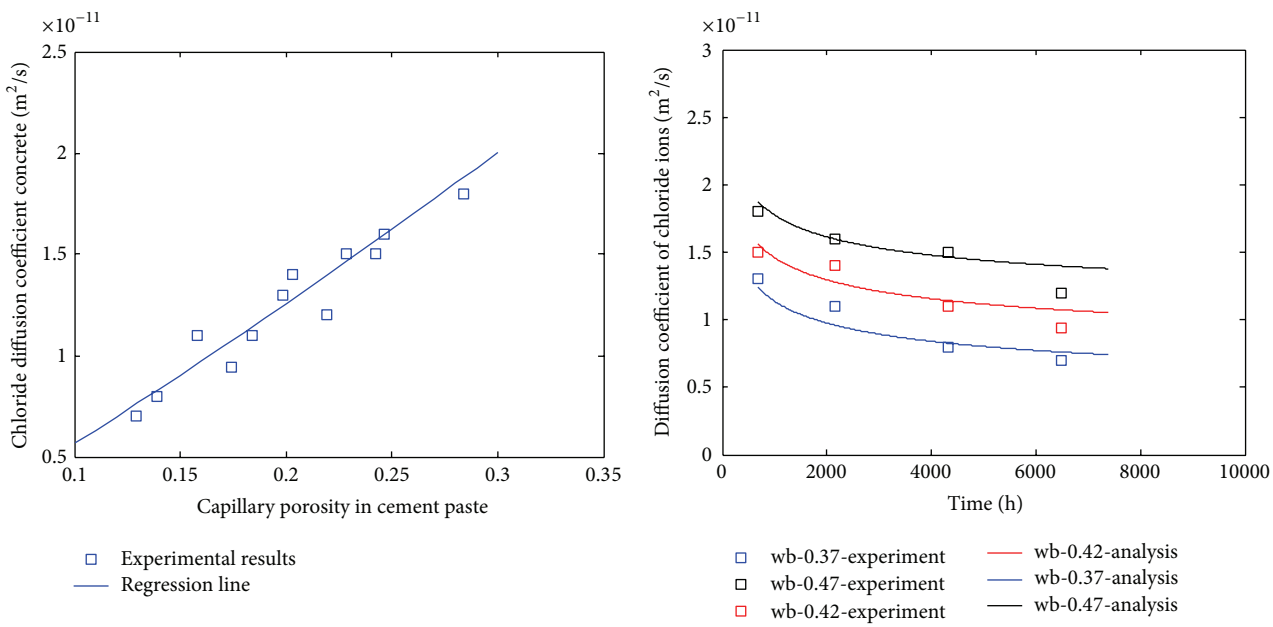

(a) Relation between capillary porosity in paste and chloride diffusion coefficients

(b) Chloride diffusion coefficients as functions of curing time

Figure 5: Evaluation of chloride ions diffusion coefficients.

dependences of chloride diffusivity and chloride binding capacity on age of concrete are clarified. Chloride diffusivity of hardening concrete is calculated considering capillary porosity evolution in cement paste and aggregate dilution effect. Chloride binding is described using nonlinear binding isotherm. Third, by using numerical analysis method, chloride profiles in hardening concrete are calculated. Analysis results generally agree with experimental results of concrete with different curing ages and different mixing proportions.

Conflict of Interests

The authors declare that there is no conflict of interests regarding the publication of this paper.

Acknowledgment

This paper is financially supported by National Research Foundation of Korea (Grant no. NRF-2013R1A1A2060231; Project name: An Integrated Program for Predicting Chloride

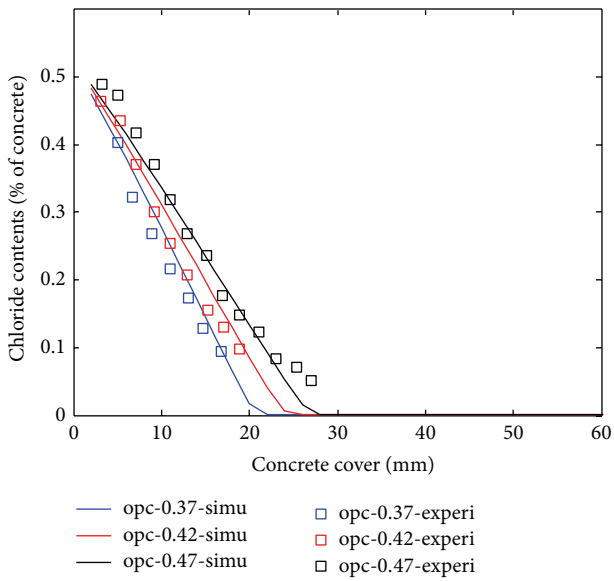

Figure 6: Chloride ions profiles in concrete.

Penetration into Reinforced Concrete Structures by Using a Cement Hydration Model).

References

[1] P. K. Metha and P. J. M. Monteiro, *Concrete: Microstructure, Properties and Materials*, McGraw-Hill, New York, NY, USA, 3rd edition, 2006.

[2] V. G. Papadakis, M. N. Fardis, and C. G. Vayenas, "Physicochemical processes and mathematical modeling of concrete chlorination," *Chemical Engineering Science*, vol. 51, no. 4, pp. 505–513, 1996.

[3] V. G. Papadakis, "Effect of supplementary cementing materials on concrete resistance against carbonation and chloride ingress," *Cement and Concrete Research*, vol. 30, no. 2, pp. 291–299, 2000.

[4] S.-H. Han, "Influence of diffusion coefficient on chloride ion penetration of concrete structure," *Construction and Building Materials*, vol. 21, no. 2, pp. 370–378, 2007.

[5] P. Spiesz, M. M. Ballari, and H. J. H. Brouwers, "RCM: a new model accounting for the non-linear chloride binding isotherm and the non-equilibrium conditions between the free- and bound-chloride concentrations," *Construction and Building Materials*, vol. 27, no. 1, pp. 293–304, 2012.

[6] P. Spiesz and H. J. H. Brouwers, "The apparent and effective chloride migration coefficients obtained in migration tests," *Cement and Concrete Research*, vol. 48, pp. 116–127, 2013.

[7] C. C. Yang, "On the relationship between pore structure and chloride diffusivity from accelerated chloride migration test in cement-based materials," *Cement and Concrete Research*, vol. 36, no. 7, pp. 1304–1311, 2006.

[8] H.-W. Song and S.-J. Kwon, "Evaluation of chloride penetration in high performance concrete using neural network algorithm and micro pore structure," *Cement and Concrete Research*, vol. 39, no. 9, pp. 814–824, 2009.

[9] T. LuPing, L.-O. Nilsson, and P. A. M. Basheer, *Resistance of Concrete to Chloride Ingress, Testing and Modeling*, Spon Press, London, UK, 2012.

[10] X.-Y. Wang and H.-S. Lee, "Modeling the hydration of concrete incorporating fly ash or slag," *Cement and Concrete Research*, vol. 40, no. 7, pp. 984–996, 2010.

[11] X.-Y. Wang, *A hydration-based integrated system for blended cement to predict the early-age properties and durability of concrete [Ph.D. thesis]*, Hanyang University, Seoul, Republic of Korea, 2010.

[12] F. Tomosawa, "Development of a kinetic model for hydration of cement," in *Proceedings of the 10th International Congress on the Chemistry of Cement*, pp. 51–58, Harald Justnes Publisher, Gothenburg, Sweden, 1997.

[13] B. Martín-Pérez, H. Zibara, R. D. Hooton, and M. D. A. Thomas, "A study of the effect of chloride binding on service life predictions," *Cement and Concrete Research*, vol. 30, no. 8, pp. 1215–1223, 2000.

[14] B. H. Oh and S. Y. Jang, "Prediction of diffusivity of concrete based on simple analytic equations," *Cement and Concrete Research*, vol. 34, no. 3, pp. 463–480, 2004.

[15] K. Maekawa, R. Chaube, and T. Kishi, *Modeling of Concrete Performance: Hydration, Microstructure Formation and Mass Transport*, Routledge, London, UK, 1998.

[16] K. Maekawa, T. Ishida, and T. Kishi, *Multi-Scale Modeling of Structural Concrete*, Taylor & Francis, London, UK, 2009.

[17] D. P. Bentz, O. M. Jensen, A. M. Coats, and F. P. Glasser, "Influence of silica fume on diffusivity in cement-based materials: I. Experimental and computer modeling studies on cement pastes," *Cement and Concrete Research*, vol. 30, no. 6, pp. 953–962, 2000.

[18] D. P. Bentz, "Influence of silica fume on diffusivity in cement-based materials: II. Multi-scale modeling of concrete diffusivity," *Cement and Concrete Research*, vol. 30, no. 7, pp. 1121–1129, 2000.

[19] K. van Breugel, "Numerical simulation of hydration and microstructural development in hardening cement-based materials (I) theory," *Cement and Concrete Research*, vol. 25, no. 2, pp. 319–331, 1995.

[20] K. van Breugel, "Numerical simulation of hydration and microstructural development in hardening cement-based materials: (II) applications," *Cement and Concrete Research*, vol. 25, no. 3, pp. 522–530, 1995.